

Microwave Sol-Gel Preparation of $\text{Eu}^{3+}/\text{Yb}^{3+}$ Co-doped $\text{NaBaY}(\text{MoO}_4)_3$ Particles and Upconversion Characteristics

Won-Chun Oh, Ji Soon Park, Eung Gyun Kim, Hak Su Kim,
Chang Sung Lim*

Department of Aerospace Advanced Materials & Chemical Engineering, Hanseo University, Seosan 356-706, Korea

Abstract: $\text{Eu}^{3+}/\text{Yb}^{3+}$ co-doped $\text{NaBaY}_{1-x}(\text{MoO}_4)_3$ phosphors with doping concentrations of Eu^{3+} and Yb^{3+} ($x = \text{Eu}^{3+} + \text{Yb}^{3+}$, $\text{Eu}^{3+} = 0.05, 0.1, 0.2$ and $\text{Yb}^{3+} = 0.2, 0.45$) were successfully prepared by the microwave sol-gel method; their upconversion characteristics were investigated. The microstructure of the synthesized particles showed a well-crystallized morphology with particle sizes of 2-5 μm . Under excitation at 980 nm, $\text{NaBaY}_{0.5}(\text{MoO}_4)_3:\text{Eu}_{0.05}\text{Yb}_{0.45}$ particles provided strong 475-nm emission band in the blue region, and a strong 525-nm and a weak 550-nm emission bands in the blue region, while a very weak 625-nm emission band in the red region. The Raman spectra of the doped particles showed the domination of strong peaks at higher frequencies of 790, 892, 1368 and 1438 cm^{-1} and the domination of weak peaks at lower frequencies of 326, 405 and 460 cm^{-1} induced by the disorder of the $[\text{MoO}_4]_2$ - groups with the partial substitution of Y^{3+} by Eu^{3+} and Yb^{3+} ions into the $\text{NaBaY}_{1-x}(\text{MoO}_4)_3$ crystal lattice.

Key words: Molybdate Phosphors, Microwave sol-gel, $\text{Eu}^{3+}/\text{Yb}^{3+}$ Co-doped $\text{NaBaY}(\text{MoO}_4)_3$ Upconversion

Introduction

Rare-earth activated molybdates have attracted great attention because of its spectroscopic characteristics and have evolved in terms of their applications, which show highly luminescence quantum yields, since usually more than one metastable excited state exists, multiple emissions are detected [1,2]. Recently, the synthesis and the photoluminescence characteristics of upconversion (UC) particles have attracted considerable interest since they are considered as potentially active components in new optoelectronic devices and luminescent labels for imaging and biodetection products, which could overcome the current limitations in traditional phosphor materials [3]. Double molybdate compounds of $\text{MR}_2(\text{MoO}_4)_4$ belong to a group of double alkaline earth lanthanide molybdates. With the decrease in the ionic radius of alkaline earth metal ions, it is possible for the structure of $\text{MR}_2(\text{MoO}_4)_4$ to be transformed to a highly

* Corresponding author: cslim@hanseo.ac.kr

disordered tetragonal scheelite structure from the monoclinic structure. It is possible for the trivalent rare earth ions in the disordered tetragonal-phase to be partially substituted by Eu^{3+} and Yb^{3+} ions, these ions could be effectively doped into the crystal lattices of the tetragonal phase due to the similar radii of the trivalent rare-earth ions in R^{3+} , which lead to the excellent UC photoluminescence properties [4-6]. Among lanthanide ions, the Eu^{3+} ion as an activator and Yb^{3+} ion as a sensitizer are suitable for converting infrared to visible light through the UC process due to its appropriate electronic energy level. The co-doped system of Eu^{3+} ion and Yb^{3+} ion can remarkably enhance the UC efficiency for the shift from infrared to visible light due to the highly effective efficiency of the energy transfer (ET) from Yb^{3+} to Eu^{3+} . The Yb^{3+} ion, as a sensitizer, can be effectively excited by an incident light source energy. This energy is transferred to the activator of Eu^{3+} ion from which radiation can be emitted [7-9].

To prepare these rare-earth doped molybdates several processes have been developed and investigated. Usually, the sol-gel method shows some advantages over the conventional solid-state method, providing good homogeneity, low calcination temperature, small particle size and narrow particle size distribution optimal. However, the sol-gel method has a disadvantage in that it takes a long time for gelation. Microwave synthesis provides the advantages of a very short process time with small-size particles, narrow particle size distribution, and high purity for final products. Microwave heating is transferred to the material surface by radiant and/or convection heating, which heat energy is delivered to the bulk of the material via conduction [10,11]. Especially, microwave sol-gel process is a highly effective method to provide high homogeneity and high purity of final products with a conventional process; it is a viable new process for the quick synthesis to prepare the high-quality luminescent materials [12,13]. However, synthesis of $\text{Eu}^{3+}/\text{Yb}^{3+}$ co-doped $\text{NaBaY}_{1-x}(\text{MoO}_4)_3$ phosphors via the microwave sol-gel route has not yet been reported.

In this study, $\text{Eu}^{3+}/\text{Yb}^{3+}$ co-doped $\text{NaBaY}_{1-x}(\text{MoO}_4)_3$ phosphors with doping concentrations of Eu^{3+} and Yb^{3+} ($x = \text{Eu}^{3+} + \text{Yb}^{3+}$, $\text{Eu}^{3+} = 0.05, 0.1, 0.2$ and $\text{Yb}^{3+} = 0.2, 0.45$) phosphors were prepared by the microwave sol-gel method. The characterization of the synthesized particles were evaluated by X-ray diffraction (XRD), scanning electron microscopy (SEM), and energy-dispersive X-ray spectroscopy (EDS). The upconversion and spectroscopic properties were investigated comparatively using photoluminescence (PL) emission and Raman spectroscopy.

Experimental

For the starting materials, stoichiometric amounts of $\text{Na}_2\text{MoO}_4 \cdot 2\text{H}_2\text{O}$ (99 %, Sigma-Aldrich, USA), $\text{Ba}(\text{NO}_3)_2$ (99%, Sigma-Aldrich, USA), $\text{Y}(\text{NO}_3)_3 \cdot 6\text{H}_2\text{O}$ (99 %, Sigma-Aldrich, USA), $(\text{NH}_4)_6\text{Mo}_7\text{O}_{24} \cdot 4\text{H}_2\text{O}$ (99%, Alfa Aesar, USA), $\text{Eu}(\text{NO}_3)_3 \cdot 5\text{H}_2\text{O}$ (99.9%, Sigma-Aldrich, USA), $\text{Yb}(\text{NO}_3)_3 \cdot 5\text{H}_2\text{O}$ (99.9%, Sigma-Aldrich, USA), citric acid (99.5%, Daejung Chemicals, Korea), NH_4OH (A.R.), ethylene glycol (A.R.) and distilled water were used to prepare $\text{NaBaY}(\text{MoO}_4)_3$, $\text{NaBaY}_{0.8}(\text{MoO}_4)_3:\text{Eu}_{0.2}$, $\text{NaBaY}_{0.7}(\text{MoO}_4)_3:\text{Eu}_{0.1}\text{Yb}_{0.2}$ and $\text{NaBaY}_{0.5}(\text{MoO}_4)_3:\text{Eu}_{0.05}\text{Yb}_{0.45}$ compounds with doping concentrations of Eu^{3+} and Yb^{3+} ($\text{Eu}^{3+} = 0.05, 0.1, 0.2$ and $\text{Yb}^{3+} = 0.2, 0.45$). To prepare $\text{NaBaY}(\text{MoO}_4)_3$, 0.2 mol% $\text{Na}_2\text{MoO}_4 \cdot 2\text{H}_2\text{O}$ and 0.143 mol% $(\text{NH}_4)_6\text{Mo}_7\text{O}_{24} \cdot 4\text{H}_2\text{O}$ were dissolved in 20 mL of

ethylene glycol and 80 mL of 5M NH_4OH . Subsequently, 0.4 mol% $\text{Ba}(\text{NO}_3)_2$ and citric acid (with a molar ratio of citric acid to total metal ions of 2:1) were dissolved in 100 mL of distilled water with vigorous stirring and heating. Then, the solutions were mixed together under vigorous stirring and heating at 80-100°C. Finally, highly transparent solutions were obtained and adjusted to pH=7-8 by the addition of NH_4OH or citric acid. In order to prepare $\text{NaBaY}_{0.8}(\text{MoO}_4)_3:\text{Eu}_{0.2}$, the mixture of 0.32 mol% $\text{Y}(\text{NO}_3)_3 \cdot 6\text{H}_2\text{O}$ with 0.08 mol% $\text{Eu}(\text{NO}_3)_3 \cdot 5\text{H}_2\text{O}$ was used for the creation of the rare earth solution. In order to prepare $\text{NaBaY}_{0.7}(\text{MoO}_4)_3:\text{Eu}_{0.1}\text{Yb}_{0.2}$, the mixture of 0.28 mol% $\text{Y}(\text{NO}_3)_3 \cdot 6\text{H}_2\text{O}$ with 0.04 mol% $\text{Eu}(\text{NO}_3)_3 \cdot 5\text{H}_2\text{O}$ and 0.08 mol% $\text{Yb}(\text{NO}_3)_3 \cdot 5\text{H}_2\text{O}$ was used for the creation of the rare earth solution. In order to prepare $\text{NaBaY}_{0.5}(\text{MoO}_4)_3:\text{Eu}_{0.05}\text{Yb}_{0.45}$, the rare earth containing solution was generated using 0.2 mol% $\text{Y}(\text{NO}_3)_3 \cdot 6\text{H}_2\text{O}$ with 0.02 mol% $\text{Eu}(\text{NO}_3)_3 \cdot 5\text{H}_2\text{O}$ and 0.18 mol% $\text{Yb}(\text{NO}_3)_3 \cdot 5\text{H}_2\text{O}$.

The transparent solutions were located for 30 min into a microwave oven operating at a frequency of 2.45 GHz for a maximum output-power of 1250 W. The microwave process for the working cycle was controlled very precisely using a regime of 40 s on and 20 s off for 15 min, and further treated using a regime of 30 s on and 30 s off for 15 min. The products were treated under ultrasonic radiation for 10 min to provide a light yellow transparent sol. After this, the light yellow transparent sols were dried at 120°C in a dry oven to obtain black dried gels. The black dried gels were ground and heat-treated at 900°C for 16 h with 100°C intervals between 600-900°C. Finally, white particles were obtained for $\text{NaBaY}(\text{MoO}_4)_3$ and pink particles were obtained for the $\text{Eu}^{3+}/\text{Yb}^{3+}$ co-doped $\text{NaBaY}_{1-x}(\text{MoO}_4)_3$.

The phase identification of the synthesized particles was evaluated using XRD (D/MAX 2200, Rigaku, Japan). The crystallized microstructure and surface morphology of the synthesized particles were observed using SEM/EDS (JSM-5600, JEOL, Japan). The PL spectra were measured using a spectrophotometer (Perkin Elmer LS55, UK) at room temperature. Raman spectroscopic properties were investigated using a LabRam Aramis (Horiba Jobin-Yvon, France). The 514.5-nm line of an Ar ion laser was used as the excitation source; the power on the samples was kept at 0.5 mW.

Results and Discussion

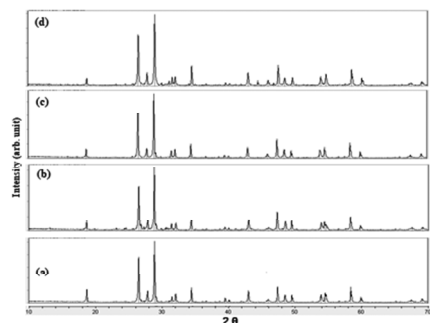


Fig. 1: X-ray diffraction patterns of the synthesized (a) $\text{NaBaY}(\text{MoO}_4)_3$, (b) $\text{NaBaY}_{0.8}(\text{MoO}_4)_3:\text{Eu}_{0.2}$, (c) $\text{NaBaY}_{0.7}(\text{MoO}_4)_3:\text{Eu}_{0.1}\text{Yb}_{0.2}$ and (d) $\text{NaBaY}_{0.5}(\text{MoO}_4)_3:\text{Eu}_{0.05}\text{Yb}_{0.45}$ particles.

Fig. 1 shows the X-ray diffraction patterns of the synthesized (a) $\text{NaBaY}(\text{MoO}_4)_3$, (b) $\text{NaBaY}_{0.8}(\text{MoO}_4)_3:\text{Eu}_{0.2}$, (c) $\text{NaBaY}_{0.7}(\text{MoO}_4)_3:\text{Eu}_{0.1}\text{Yb}_{0.2}$, and (d) $\text{NaBaY}_{0.5}(\text{MoO}_4)_3:\text{Eu}_{0.05}\text{Yb}_{0.45}$ particles. No impurity phases were detected. $\text{NaBaY}(\text{MoO}_4)_3$ as a member of triple molybdate family is tetragonal with a space group $I4_1/a$. Post heat-treatment provides an important result in a well-defined crystallized morphology. To achieve a well-defined crystalline morphology, the phases are required to be heat treated at 900°C for 16 h. It is noted that the doping amount of $\text{Eu}^{3+}/\text{Yb}^{3+}$ provides a great effect on the crystalline cell volume of the $\text{NaBaY}(\text{MoO}_4)_3$, because of the different ionic sizes. The co-doped system of Eu^{3+} ion and Yb^{3+} ion can remarkably enhance the UC efficiency due to the highly effective efficiency of the energy transfer (ET) from Yb^{3+} to Eu^{3+} . It should be emphasized that that the synthesized $\text{Eu}^{3+}/\text{Yb}^{3+}$ co-doped $\text{NaBaY}(\text{MoO}_4)_3$ with a tetragonal-phase after partial substitution of Y^{3+} and by Eu^{3+} and Yb^{3+} ions and that the ions are effectively doped into the $\text{NaBaY}(\text{MoO}_4)_3$ crystal lattice because of the similar radii of Y^{3+} , Eu^{3+} and Yb^{3+} .

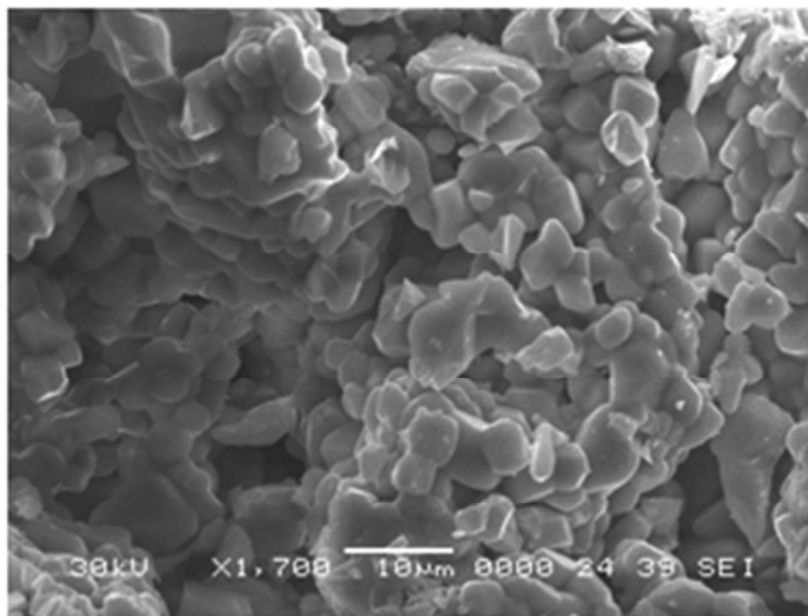


Fig. 2: Scanning electron microscopy image of the synthesized $\text{NaBaY}_{0.5}(\text{MoO}_4)_3:\text{Eu}_{0.05}\text{Yb}_{0.45}$ particles.

Fig. 2 shows a SEM image of the synthesized $\text{Eu}_{0.05}/\text{Yb}_{0.45}$ co-doped $\text{NaBaY}_{0.5}(\text{MoO}_4)_3$ particles. The synthesized sample shows well crystallized morphology with particle sizes of 2-5 μm . It is noted that the obtained sample possesses a partial substitution of Y^{3+} by Eu^{3+} and Yb^{3+} ions, and the ions are effectively doped into crystal lattices of the $\text{NaBaY}(\text{MoO}_4)_3$ phase due to the similar radii of Y^{3+} and by Eu^{3+} and Yb^{3+} . This suggests that the microwave sol-gel route is suitable for the growth of $\text{Eu}^{3+}/\text{Yb}^{3+}$ co-doped $\text{NaBaY}_{1-x}(\text{MoO}_4)_3$ crystallites.

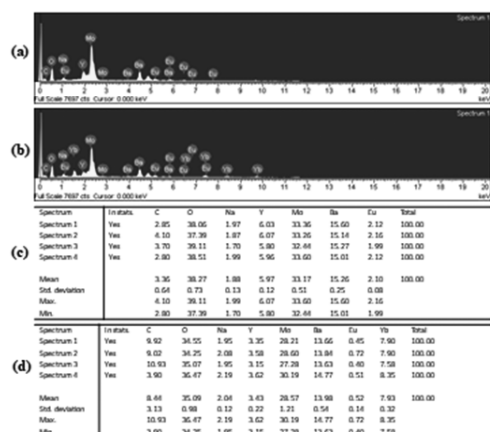


Fig. 3: Energy-dispersive X-ray spectroscopy patterns of the synthesized (a) $\text{NaBaY}_{0.8}(\text{MoO}_4)_2:\text{Eu}_{0.2}$ and (b) $\text{NaBaY}_{0.5}(\text{MoO}_4)_2:\text{Eu}_{0.05}\text{Yb}_{0.45}$ particles, and quantitative compositions of (c) $\text{NaBaY}_{0.8}(\text{MoO}_4)_2:\text{Eu}_{0.2}$ and (d) $\text{NaBaY}_{0.5}(\text{MoO}_4)_2:\text{Eu}_{0.05}\text{Yb}_{0.45}$ particles.

Fig. 3 shows the energy-dispersive X-ray spectroscopy patterns of the synthesized (a) $\text{NaBaY}_{0.8}(\text{MoO}_4)_2:\text{Eu}_{0.2}$ and (b) $\text{NaBaY}_{0.5}(\text{MoO}_4)_2:\text{Eu}_{0.05}\text{Yb}_{0.45}$ particles, and quantitative compositions of (c) $\text{NaBaY}_{0.8}(\text{MoO}_4)_2:\text{Eu}_{0.2}$ and (d) $\text{NaBaY}_{0.5}(\text{MoO}_4)_2:\text{Eu}_{0.05}\text{Yb}_{0.45}$ particles. The EDS pattern shows that the (a) $\text{NaBaY}_{0.8}(\text{MoO}_4)_2:\text{Eu}_{0.2}$ and (b) $\text{NaBaY}_{0.5}(\text{MoO}_4)_2:\text{Eu}_{0.05}\text{Yb}_{0.45}$ particles are composed of Na, Ba, Y, Mo, O and Eu for $\text{NaBaY}_{0.8}(\text{MoO}_4)_2:\text{Eu}_{0.2}$ and Na, Ba, Y, Mo, O, Eu and Yb for $\text{NaBaY}_{0.5}(\text{MoO}_4)_2:\text{Eu}_{0.05}\text{Yb}_{0.45}$ particles. The quantitative compositions of (c) and (d) are in good relation with nominal compositions of the particles. The relation of Na, Ba, Y, Mo, O, Eu and Yb components exhibits that the microwave sol-gel method is suitable for the preparation of $\text{NaBaY}_{0.8}(\text{MoO}_4)_2:\text{Eu}_{0.2}$ and $\text{NaBaY}_{0.5}(\text{MoO}_4)_2:\text{Eu}_{0.05}\text{Yb}_{0.45}$ particles. The microwave sol-gel process of triple molybdate is a viable new approach for the quick synthesis to prepare the high-quality upconversion phosphors uniformly.

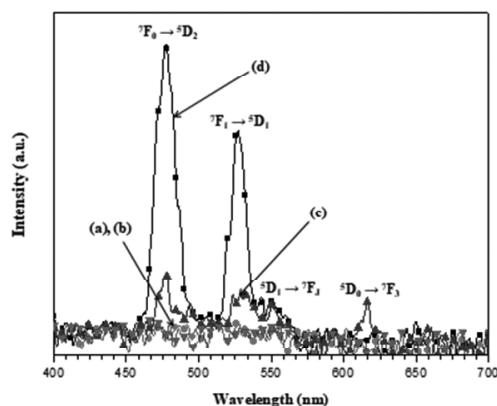


Fig. 4: Upconversion photoluminescence emission spectra of (a) $\text{NaBaY}(\text{MoO}_4)_3$, (b) $\text{NaBaY}_{0.8}(\text{MoO}_4)_3:\text{Eu}_{0.2}$, (c) $\text{NaBaY}_{0.7}(\text{MoO}_4)_3:\text{Eu}_{0.1}\text{Yb}_{0.2}$ and (d) $\text{NaBaY}_{0.5}(\text{MoO}_4)_3:\text{Eu}_{0.05}\text{Yb}_{0.45}$ particles excited under 980 nm at room temperature.

Fig. 4 shows the UC photoluminescence emission spectra of the as-prepared of (a) $\text{NaBaY}(\text{MoO}_4)_3$, (b) $\text{NaBaY}_{0.8}(\text{MoO}_4)_3:\text{Eu}_{0.2}$, (c) $\text{NaBaY}_{0.7}(\text{MoO}_4)_3:\text{Eu}_{0.1}\text{Yb}_{0.2}$, and (d) $\text{NaBaY}_{0.5}(\text{MoO}_4)_3:\text{Eu}_{0.05}\text{Yb}_{0.45}$ particles excited under 980 nm at room temperature. The UC intensities of (d) $\text{NaBaY}_{0.5}(\text{MoO}_4)_3:\text{Eu}_{0.05}\text{Yb}_{0.45}$ particles showed a strong 475-nm emission band in the blue region, and a strong 525-nm and a weak 550-nm emission bands in the green region. The UC intensities of (c) $\text{NaBaY}_{0.7}(\text{MoO}_4)_3:\text{Eu}_{0.1}\text{Yb}_{0.2}$ particles exhibited a weak 475-nm emission band in the blue region and weak 525- and 550-nm emission bands in the green region, and a weak 625-nm emission band in the red region. The strong 475-nm emission band in the blue region and the strong 525-nm emission band in the green region were assigned to the ${}^7\text{F}_0 \rightarrow {}^5\text{D}_2$ transition and the ${}^7\text{F}_1 \rightarrow {}^5\text{D}_1$ transition, respectively. The weak 550-nm emission band in the green region and the weak 625-nm emission band in the red region were assigned to the ${}^5\text{D}_1 \rightarrow {}^7\text{F}_1$ transition and the ${}^5\text{D}_0 \rightarrow {}^7\text{F}_3$ transition, respectively. The UC intensities of (a) $\text{NaBaY}(\text{MoO}_4)_3$ and (b) $\text{NaBaY}_{0.8}(\text{MoO}_4)_3:\text{Eu}_{0.2}$ were not detected. The UC intensity of (d) $\text{NaBaY}_{0.5}(\text{MoO}_4)_3:\text{Eu}_{0.05}\text{Yb}_{0.45}$ is much higher than that of (c) $\text{NaBaY}_{0.7}(\text{MoO}_4)_3:\text{Eu}_{0.1}\text{Yb}_{0.2}$ particles. The doping amounts of $\text{Eu}^{3+}/\text{Yb}^{3+}$ were affected on the crystallized morphology of the phosphors and their UC photoluminescent intensity. The Yb^{3+} ion as a sensitizer can be effectively excited by the energy of an incident light source, this energy is transferred to the Eu^{3+} activator where radiation can be emitted. Therefore, the Eu^{3+} ion activator is the luminescence center for these UC particles to be emitted, and the sensitizer Yb^{3+} leads to the enhancement of the UC luminescence efficiency [14,15].

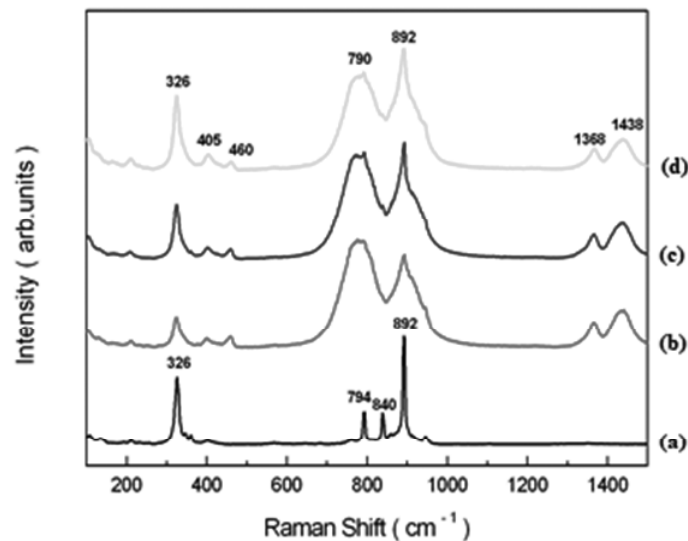


Fig. 5: Raman spectra of the synthesized (a) $\text{NaBaY}(\text{MoO}_4)_3$, (b) $\text{NaBaY}_{0.8}(\text{MoO}_4)_3:\text{Eu}_{0.2}$, (c) $\text{NaBaY}_{0.7}(\text{MoO}_4)_3:\text{Eu}_{0.1}\text{Yb}_{0.2}$, and (d) $\text{NaBaY}_{0.5}(\text{MoO}_4)_3:\text{Eu}_{0.05}\text{Yb}_{0.45}$ particles excited by the 514.5-nm line of an Ar ion laser at 0.5 mW.

Fig. 5 shows the Raman spectra of the synthesized Raman spectra of the synthesized (a) $\text{NaBaY}(\text{MoO}_4)_3$, (b) $\text{NaBaY}_{0.8}(\text{MoO}_4)_3:\text{Eu}_{0.2}$, (c) $\text{NaBaY}_{0.7}(\text{MoO}_4)_3:\text{Eu}_{0.1}\text{Yb}_{0.2}$ and (d) $\text{NaBaY}_{0.5}(\text{MoO}_4)_3:\text{Eu}_{0.05}\text{Yb}_{0.45}$ particles excited by the 514.5-nm line of an Ar ion laser at 0.5 mW. The internal modes for the (a) $\text{NaBaY}(\text{MoO}_4)_3$ particles were detected at 326, 794, 840 and 892 cm^{-1} , respectively. The well-resolved peaks for the $\text{NaBaY}(\text{MoO}_4)_3$ particles provide a high crystallinity state of the synthesized phosphors. The internal vibration mode frequencies play an important role to identify the lattice parameters and the degree of the partially covalent bond between the cation and the molecular ionic group. The Raman spectra of the doped particles indicated the domination of strong peaks at higher frequencies of 790, 892, 1368 and 1438 cm^{-1} and the domination of weak peaks at lower frequencies of 326, 405 and 460 cm^{-1} . The co-doped particles prove that the doping ions can affect the structure of the host materials. The combination of a heavy metal cation and the inter-ionic distance for Eu^{3+} and Yb^{3+} substitutions in Y^{3+} sites in the lattice results in symmetric stretching vibration and crystal structure modulation of the M-O in $\text{Eu}^{3+}/\text{Yb}^{3+}$ co-doped $\text{NaBaY}_{1-x}(\text{MoO}_4)_2:\text{Eu}^{3+}/\text{Yb}^{3+}$ crystals. It is assumed that these very strong and strange effects are generated by the disorder of the $[\text{MoO}_4]^{2-}$ groups with the incorporation of the Eu^{3+} and Yb^{3+} elements into the crystal lattice [16].

Conclusions

$\text{Eu}^{3+}/\text{Yb}^{3+}$ co-doped $\text{NaBaY}_{1-x}(\text{MoO}_4)_2$ phosphors with doping concentrations of Eu^{3+} and Yb^{3+} ($x = \text{Eu}^{3+} + \text{Yb}^{3+}$, $\text{Er}^{3+} = 0.05, 0.1, 0.2$ and $\text{Yb}^{3+} = 0.2, 0.45$) were successfully synthesized by the microwave sol-gel method. The microstructure of the synthesized particles showed a well crystallized morphology with particle sizes of 2-5 μm . Under excitation at 980 nm, the UC intensities of $\text{NaBaY}_{0.5}(\text{MoO}_4)_2:\text{Eu}_{0.05}\text{Yb}_{0.45}$ particles showed a strong 475-nm emission band in the blue region, and a strong 525-nm and a weak 550-nm emission bands in the green region. The strong 475-nm emission band in the blue region and the strong 525-nm emission band in the green region were assigned to the ${}^7\text{F}_0 \rightarrow {}^5\text{D}_2$ transition and the ${}^7\text{F}_1 \rightarrow {}^5\text{D}_1$ transition, respectively. The weak 550-nm emission band in the green region and the weak 625-nm emission band in the red region were assigned to the ${}^5\text{D}_1 \rightarrow {}^7\text{F}_1$ transition and the ${}^5\text{D}_0 \rightarrow {}^7\text{F}_3$ transition, respectively. The Raman spectra of the doped particles indicated the domination of strong peaks at higher frequencies of 790, 892, 1368 and 1438 cm^{-1} and the domination of weak peaks at lower frequencies of 326, 405 and 460 cm^{-1} .

Acknowledgment

This research was supported by the Basic Science Research Program through the National Research Foundation of Korea (NRF) funded by the Ministry of Science, ICT and future Planning (2018R1D1A1A09082321).

References

1. M. Lin, Y. Zho, S. Wang, M. Liu, Z. Duan, Y. Chen, F. Li, F. Xu, T. Lu, *Bio. Adv.*, 30, 1551 (2012).
2. M. Wang, G. Abbineni, A. Clevenger, C. Mao, S. Xu, *Nanomed.* 7, 710 (2011).

3. A. Shalav, B.S. Richards, M.A. Green, *Sol. Ener. Mater. Sol. Cells*, 91, 829 (2007).
4. C. Guo, H. K. Yang, J.H. Jeong, *J. Lumin.*, 130, 1390 (2010).
5. J. Liao, D. Zhou, B. Yang, R. liu, Q. Zhang, Q. Zhou, *J. Lumin.*, 134, 533 (2013).
6. J. Sun, J. Xian, H. Du, *J. Phys. Chem. Solids*, 72, 207 (2011).
7. T. Li, C. Guo, Y. Wu, L. Li, J.H. Jeong, *J. Alloys Comp.*, 540, 107 (2012).
8. M. Nazarov, D.Y. Noh, *J. Rare Earths*, 28, 1 (2010).
9. J. Sun, W. Zhang, W. Zhang, H. Du, *Mater. Res. Bull.*, 47, 786 (2012).
10. S. Das, A.K. Mukhopadhyay, S. Datta, D. Basu, *Bull. Mater. Sci.*, 32, 1 (2009).
11. T. Thongtem, A. Phuruangrat, S. Thongtem, *J. Nanopart. Res.*, 12, 2287 (2010) .
12. C.S. Lim, *Mater. Res. Bull.*, 60, 537 (2014).
13. C.S. Lim, *Infr. Phys. Tech.*, 67, 371 (2014).
14. J. Sun , J. Xian, X. Zhang, H. Du, *J. Rare Earths*, 29, 32 (2011).
15. Q. Sun X. Chen, Z. Liu, F. Wang, Z. Jiang, C. Wang, *J. Alloys Comp.*, 509, 5336 (2012).
16. C.S. Lim, *Mater. Res. Bull.*, 48, 3805 (2013).